

Copy  
RM L50E12

NACA RM L50E12

**CHANGED**

UNCLASSIFIED<sup>20</sup>

ot

By authority of ~~the~~

85-21812-58

that experience

# NACA

# RESEARCH MEMORANDUM

AN INVESTIGATION OF A SUPERSONIC AIRCRAFT CONFIGURATION  
HAVING A TAPERED WING WITH CIRCULAR-ARC  
SECTIONS AND 40° SWEEPBACK

## STATIC LONGITUDINAL STABILITY AND CONTROL CHARACTERISTICS

AT A MACH NUMBER OF 1.59

By M. Leroy Spearman and John H. Hilton, Jr.

Langley Aeronautical Laboratory  
Langley Air Force Base, Va.

CLASSIFIED DOCUMENT

This document contains classified information affecting the National Defense of the United States within the meaning of the Espionage Act, USC 50131 and 52. Its transmission or the revelation of its contents in any manner to an unauthorized person is prohibited by law. Information so classified may be imparted only to persons in the military and naval service of the United States, appropriate civilian officers and employees of the Federal Government who have a legitimate interest therein, and to United States citizens of known loyalty and discretion who of necessity must be informed thereof.

NATIONAL ADVISORY COMMITTEE  
FOR AERONAUTICS

WASHINGTON

June 29, 1950

~~CONFIDENTIAL~~

NATIONAL ADVISORY COMMITTEE FOR AERONAUTICS

RESEARCH MEMORANDUM

AN INVESTIGATION OF A SUPERSONIC AIRCRAFT CONFIGURATION  
HAVING A TAPERED WING WITH CIRCULAR-ARC  
SECTIONS AND  $40^\circ$  SWEEPBACK  
STATIC LONGITUDINAL STABILITY AND CONTROL CHARACTERISTICS  
AT A MACH NUMBER OF 1.59

By M. Leroy Spearman and John H. Hilton, Jr.

SUMMARY

An investigation has been conducted in the Langley 4- by 4-foot supersonic tunnel to determine the static longitudinal stability and control characteristics of a supersonic aircraft configuration at a Mach number of 1.59 and a Reynolds number of approximately 575,000 based on the mean aerodynamic chord. The model had a  $40^\circ$  sweptback tapered wing with 10-percent-thick circular-arc sections normal to the quarter-chord line.

The results showed a high degree of static longitudinal stability throughout the lift-coefficient range investigated.

In comparison with the results obtained for the same model at a Mach number of 1.40, the results at a Mach number of 1.59 showed a lower maximum trim lift coefficient (0.35 compared with 0.38) but slightly greater maneuverability. Although the difference in static longitudinal stability was small, the model appeared slightly less stable at a Mach number of 1.59.

INTRODUCTION

A comprehensive wind-tunnel investigation has been conducted in the Langley 4- by 4-foot supersonic tunnel to determine the stability and

control characteristics and the general aerodynamic characteristics of a supersonic aircraft configuration. The static longitudinal stability and control characteristics at a Mach number of 1.40 are presented in reference 1 and the static lateral stability characteristics at Mach numbers of 1.40 and 1.59 have been presented in reference 2. The pressures over the fuselage are given in reference 3 and 4 for Mach numbers of 1.59 and 1.40, respectively, and the pressures over the wing are given in reference 5 for a Mach number of 1.59. The present paper presents the results of the static longitudinal stability and control investigation at a Mach number of 1.59 and a comparison is made with the results obtained at a Mach number of 1.40 (reference 1).

### COEFFICIENTS AND SYMBOLS

The results of the tests are presented as standard NACA coefficients of forces and moments. The data are referred to the stability axes (fig. 1) with the reference center of gravity at 25 percent of the mean aerodynamic chord.

The coefficients and symbols are defined as follows:

$C_L$	lift coefficient ( $Lift/qS$ where $lift = -Z$ )
$C_D$	drag coefficient ( $Drag/qS$ where $drag = -X$ )
$C_m$	pitching-moment coefficient ( $M'/qS\bar{c}$ )
$C_{h_t}$	stabilizer hinge-moment coefficient ( $H_t/qS_t\bar{c}_t$ )
$Z$	force along Z-axis, pounds
$X$	force along X-axis, pounds
$M'$	moment about Y-axis, pound-feet
$H_t$	stabilizer hinge moment, measured about 21-percent station of stabilizer mean aerodynamic chord, pound-feet
$q$	free-stream dynamic pressure, pounds per square foot
$M$	Mach number
$S$	wing area, square feet
$S_t$	stabilizer area, square feet

$\bar{c}$	wing mean aerodynamic chord, feet $\left( \frac{2}{S} \int_0^{b/2} c^2 dy \right)$
$c$	airfoil section chord, feet
$b$	wing span, feet
$y$	distance along wing span, feet
$\bar{c}_t$	stabilizer mean aerodynamic chord, feet
$\alpha$	angle of attack of fuselage center line, degrees
$i_t$	stabilizer incidence angle with respect to fuselage center line, degrees
$\epsilon$	effective angle of downwash, degrees
$C_{m_t}$	increment of pitching-moment coefficient provided by the tail
$L/D$	ratio of lift to drag ( $C_L/C_D$ )
$W/S$	wing loading, pounds per square foot
$\partial C_m / \partial i_t$	stabilizer effectiveness, rate of change of pitching-moment coefficient with stabilizer incidence angle
$\partial \epsilon / \partial \alpha$	rate of change of effective downwash angle with angle of attack
$C_{L_\alpha}$	trim-lift-curve slope for complete model
$\partial C_m / \partial C_L$	rate of change of pitching-moment coefficient with lift coefficient
$\left( \frac{\partial C_m}{\partial C_L} \right)_0$	rate of change of pitching-moment coefficient with lift coefficient for the tail-off configuration
$C_{h_\alpha}$	rate of change of stabilizer hinge-moment coefficient with angle of attack for constant stabilizer incidence angle $\left( \partial C_{h_t} / \partial \alpha \right)_{i_t}$

- $C_{h\delta}$  rate of change of stabilizer hinge-moment coefficient with stabilizer incidence angle for constant angle of attack  
 $(\partial C_{h_t} / \partial i_t)_{\alpha}$
- $g$  acceleration due to gravity

#### MODEL AND APPARATUS

A three-view drawing of the model is shown in figure 2 and the geometric characteristics are presented in table I. The model is shown mounted in the tunnel in figure 3.

The model had a wing sweptback  $40^\circ$  at the quarter-chord line, an aspect ratio of 4, a taper ratio of 0.5, and 10-percent-thick circular-arc sections normal to the quarter-chord line. Flat-sided 20-percent-chord ailerons having a trailing-edge thickness 0.5 of the hinge-line thickness were installed on the outboard 50 percent of the wing semispans.

The model was mounted on a sting support. The angle in the horizontal plane (angle of attack) was changed in such a manner that the model remained essentially in the center of the test section. The stabilizer angle was remotely controlled by means of an electric motor mounted inside the model fuselage.

Forces and moments of the model were measured by means of a six-component strain-gage balance housed within the model. Individual strain-gage balances were mounted on the control surfaces for the determination of the control-surface hinge moments.

The tests were conducted in the Langley 4- by 4-foot supersonic tunnel which is described in reference 3.

#### TESTS

##### Test Conditions

The tests were conducted at a Mach number of 1.59 and a Reynolds number of approximately 575,000 based on the mean aerodynamic chord of 0.557 foot; the dynamic pressure was about 223 pounds per square foot. For these tests, the tunnel was operated at a stagnation pressure of 0.25 atmosphere and a stagnation temperature of  $110^\circ$  F. The stagnation dew point was maintained at  $-35^\circ$  F or less. Calibration data for the

M = 1.59 nozzle (reference 3) indicate that dew points of this magnitude are required in order to eliminate any serious condensation effects.

### Corrections and Accuracy

No corrections due to sting interference were applied to the data. Although the sting effects are believed to be small, the exact magnitude is not known. Base-pressure measurements indicated that, if free-stream static pressure is assumed to exist at the base of the model, the drag data presented would be reduced by approximately 1 percent in the angle-of-attack range from  $4^\circ$  to  $10^\circ$ , with no correction necessary in the lower-angle range.

Optical measurements of the wing twist under load indicated twists of less than  $0.05^\circ$  and, hence, no corrections for aeroelastic effects were necessary.

For the present test conditions the maximum uncertainties in the aerodynamic coefficients attributable to the balance system are:

$C_L$	±0.0010
$C_D$	±0.00025
$C_m$	±0.00045
$C_{ht}$	±0.0013

The accuracy of the angle of attack was about  $\pm 0.05^\circ$ ; the tail incidence, about  $\pm 0.10^\circ$ ; and the dynamic pressure, about 0.25 percent.

The variation in Mach number in the vicinity of the model due to flow irregularities is about  $\pm 0.01$ . The flow angularity in the horizontal plane is about  $0^\circ$  to  $0.20^\circ$  and approximately  $0.30^\circ$  to  $0^\circ$  in the vertical plane (reference 3). Tests made with the model in the vertical and horizontal positions indicated excellent agreement.

### Test Procedure

The longitudinal tests covered an angle-of-attack range from  $-4^\circ$  to  $10^\circ$  with a range of stabilizer incidence angles from  $4^\circ$  to  $-10^\circ$ . The stabilizer angles were selected to maintain conditions near trim. In addition, one test was made with the stabilizer removed (tail off).

## DISCUSSION

The variation of pitching-moment coefficient, drag coefficient, and angle of attack with lift coefficient is shown in figure 4 for the model with various stabilizer angles and with the stabilizer removed. From these data, the static longitudinal stability can be determined as well as some of the factors affecting the stability. The variation of the effective downwash angle with angle of attack and lift coefficient (fig. 5) was obtained by means of the relation  $\epsilon = \alpha + i_t - \frac{C_{m_t}}{\partial C_m / \partial i_t}$ .

The downwash trends at  $M = 1.59$  are similar to those obtained for the same model at  $M = 1.40$ , but the effective downwash angle at a given angle of attack (fig. 5(a)) is slightly lower. Although this result might be expected because of the lower lift-curve slope, the variation of the effective downwash angle with lift coefficient (fig. 5(b)) still indicates that throughout the trim lift range the effective downwash angle is slightly lower at  $M = 1.59$ . It is possible that the difference in the effective downwash angles near zero lift results from differences in body downwash in the vicinity of the tail. Unpublished calculations of the body downwash in this vicinity indicate that the downwash angle near zero lift is about a quarter of a degree lower at  $M = 1.59$  than at  $M = 1.40$ . This difference diminishes slightly with increasing angle of attack. At the higher angles of attack the effective downwash may be influenced by the wing-tip Mach cones although this effect is probably small at  $M = 1.40$  and would be still less at  $M = 1.59$ .

A summary of the variation of the longitudinal stability determinants with lift coefficient as determined from the data of figure 4 is presented in figure 6 together with the results obtained at  $M = 1.40$  (reference 1) and some results from tests conducted with a similar configuration at  $M = 0.16$  (reference 6). The relative effects of the various determinants on the stability of the complete model can be determined from an analysis of figure 6 and from the approximate relation for the total stability:

$$\frac{\partial C_m}{\partial C_L} = \left( \frac{\partial C_m}{\partial C_L} \right)_0 + \frac{\partial C_m}{\partial i_t} \left( 1 - \frac{\partial \epsilon}{\partial \alpha} \right) \frac{1}{C_{L_\alpha}}$$

As a result of the compensating effects of the various determinants, there is little variation in the stability of the complete model. For example, at  $M = 1.59$ , in the lift-coefficient range from 0.08 to 0.15, the rapid increase indicated in the stability for the model with the tail off compensates for the destabilizing effect of the increased  $\partial \epsilon / \partial \alpha$ . These antithetical effects are also evident in the results for  $M = 1.40$  (reference 1).

Although the differences in  $\partial C_m / \partial C_L$  are small (fig. 6), the complete model appears to be slightly less stable at  $M = 1.59$  than at  $M = 1.40$ . The effect of the lower lift-curve slope at  $M = 1.59$  is stabilizing throughout the lift-coefficient range while the lower stabilizer effectiveness is destabilizing. The variations in  $\partial \epsilon / \partial \alpha$  and in the tail-off  $\partial C_m / \partial C_L$  are such that their effects on the total stability tend to cancel.

At supersonic speeds, the complete model exhibits a high degree of static longitudinal stability - the static margin being about 34 percent of the mean aerodynamic chord as compared to the low-speed value of approximately 11 percent near zero lift. It is evident that this increase in stability is largely a function of the tail-off stability inasmuch as the tail-off configuration, which is unstable at low speeds, becomes quite stable at supersonic speeds. This increase in stability might be attributed to a rearward shift of the wing center of pressure and to a stabilizing wing-fuselage interference effect resulting from the fact that the wing-lift carry-over region in the presence of the fuselage acts farther downstream. This latter effect has been observed in unpublished pressure measurements of this configuration and has been mentioned in reference 5. It is interesting to note that the increment of  $\partial C_m / \partial C_L$  between the tail-off configuration and the complete model is about the same at supersonic speeds as at low speed. However, the factors comprising the tail contribution differ widely. The higher  $C_{L\alpha}$  and  $\partial \epsilon / \partial \alpha$  at low speed are destabilizing whereas the more negative  $\partial C_m / \partial i_t$  is stabilizing but the combination of these factors results in approximately the same tail contribution as that obtained at Mach numbers of 1.40 and 1.59.

The maximum trim lift coefficient obtained at  $M = 1.59$  was 0.35 (figs. 4 and 7) as compared to a value of 0.38 obtained at  $M = 1.40$  (reference 1). However, in determining the maximum normal acceleration (the ratio of the maximum trim lift coefficient to the lift coefficient required for trimmed level flight (fig. 7)) for an airplane similar to the model it was found that, for a given wing loading and altitude higher normal accelerations might be obtained at  $M = 1.59$  than at  $M = 1.40$ . This fact is shown in figure 8 for an altitude of 60,000 feet and a wing loading of 60 pounds per square foot where the maximum normal acceleration is 1.56g at  $M = 1.59$  and 1.30g at  $M = 1.40$ . This greater maneuverability results from the fact that in this Mach number range the lift coefficient required for trimmed level flight decreases with Mach number at a more rapid rate than does the maximum trim lift coefficient.

By the use of the stabilizer data (fig. 4) in conjunction with the lift coefficient required for trimmed level flight (fig. 7) and comparable data from reference 1, the stabilizer deflection required for trimmed level



flight at  $M = 1.59$  and  $M = 1.40$  was determined. The results (fig. 8) indicated stick-position stability in that a forward movement of the stick (down stabilizer) is required to maintain trimmed level flight when increasing the Mach number from 1.40 to 1.59.

The variation of stabilizer hinge-moment coefficient with lift coefficient for various stabilizer deflections is presented in figure 9 and the variation of stabilizer hinge-moment coefficient with stabilizer incidence for various angles of attack is given in figure 10. The hinge-moment parameters  $C_{h\alpha}$  and  $C_{h\delta}$  are fairly linear and indicate large hinge moments.

Through most of the lift-coefficient range, the trimmed lift-drag ratios (fig. 11) are slightly higher at  $M = 1.59$  than at  $M = 1.40$ , although approximately the same maximum value is obtained. The maximum lift-drag ratio was about 3.2 as compared to a low-speed value of about 10 (reference 6).

#### CONCLUDING REMARKS

The results of the static longitudinal stability and control investigation conducted at a Mach number of 1.59 on a model of a supersonic aircraft configuration show a high degree of longitudinal stability throughout the lift-coefficient range investigated.

In comparison with the results obtained for the same model at a Mach number of 1.40, the results at a Mach number of 1.59 show a lower maximum trim lift coefficient (0.35 compared with 0.38) but slightly greater maneuverability. Although the difference in static longitudinal stability is small, the model appears slightly less stable at a Mach number of 1.59.

Langley Aeronautical Laboratory  
National Advisory Committee for Aeronautics  
Langley Air Force Base, Va.

## REFERENCES

1. Spearman, M. Leroy: An Investigation of a Supersonic Aircraft Configuration Having a Tapered Wing with Circular-Arc Sections and  $40^\circ$  Sweepback. Static Longitudinal Stability and Control Characteristics at a Mach Number of 1.40. NACA RM L9L08, 1950.
2. Spearman, M. Leroy: An Investigation of a Supersonic Aircraft Configuration Having a Tapered Wing with Circular-Arc Sections and  $40^\circ$  Sweepback. Static Lateral Stability Characteristics at Mach numbers of 1.40 and 1.59. NACA RM L50C17, 1950.
3. Cooper, Morton, Smith, Norman F., and Kainer, Julian H.: A Pressure-Distribution Investigation of a Supersonic Aircraft Fuselage and Calibration of the Mach Number 1.59 Nozzle of the Langley 4- by 4-Foot Supersonic Tunnel. NACA RM L9E27a, 1949.
4. Hasel, Lowell E., and Sinclair, Archibald R.: A Pressure-Distribution Investigation of a Supersonic-Aircraft Fuselage and Calibration of the Mach Number 1.40 Nozzle of the Langley 4- by 4-Foot Supersonic Tunnel. NACA RM L50B14a, 1950.
5. Cooper, Morton, and Spearman, M. Leroy: An Investigation of a Supersonic Aircraft Configuration Having a Tapered Wing with Circular-Arc Sections and  $40^\circ$  Sweepback. A Pressure-Distribution Study of the Aerodynamic Characteristics of the Wing at Mach Number 1.59. NACA RM L50C24, 1950.
6. Weil, Joseph, Comisarow, Paul, and Goodson, Kenneth W.: Longitudinal Stability and Control Characteristics of an Airplane Model Having a  $42.8^\circ$  Sweptback Circular-Arc Wing with Aspect Ratio 4.00, Taper Ratio 0.50, and Sweptback Tail Surfaces. NACA RM L7G28, 1947.

TABLE 1.- GEOMETRIC CHARACTERISTICS OF MODEL

## Wing:

Area, sq ft . . . . .	1.158
Span, ft . . . . .	2.155
Aspect ratio . . . . .	4
Sweepback of quarter-chord line, deg . . . . .	40
Taper ratio . . . . .	0.5
Mean aerodynamic chord, ft . . . . .	0.557
Airfoil section normal to quarter-chord line . . . . .	10-percent-thick circular arc
Twist, deg . . . . .	0

## Horizontal tail:

Area, sq ft . . . . .	0.196
Span, ft . . . . .	0.855
Aspect ratio . . . . .	3.72
Sweepback of quarter-chord line, deg . . . . .	40
Taper ratio . . . . .	0.5
Airfoil section . . . . .	NACA 65-008

## Vertical tail:

Area (exposed), sq ft . . . . .	0.172
Aspect ratio (based on exposed area and span) . . . . .	1.17
Sweepback of leading edge, deg . . . . .	40.6
Taper ratio . . . . .	0.337
Airfoil section, root . . . . .	NACA 27-010
Airfoil section, tip . . . . .	NACA 27-008

## Fuselage:

Fineness ratio (neglecting canopies) . . . . .	9.4
--	-----

## Miscellaneous:

Tail length from $\bar{c}/4$ wing to $\bar{c}_t/4$ tail, ft . . . . .	0.917
Tail height, wing semispans above fuselage center line . . . . .	0.153



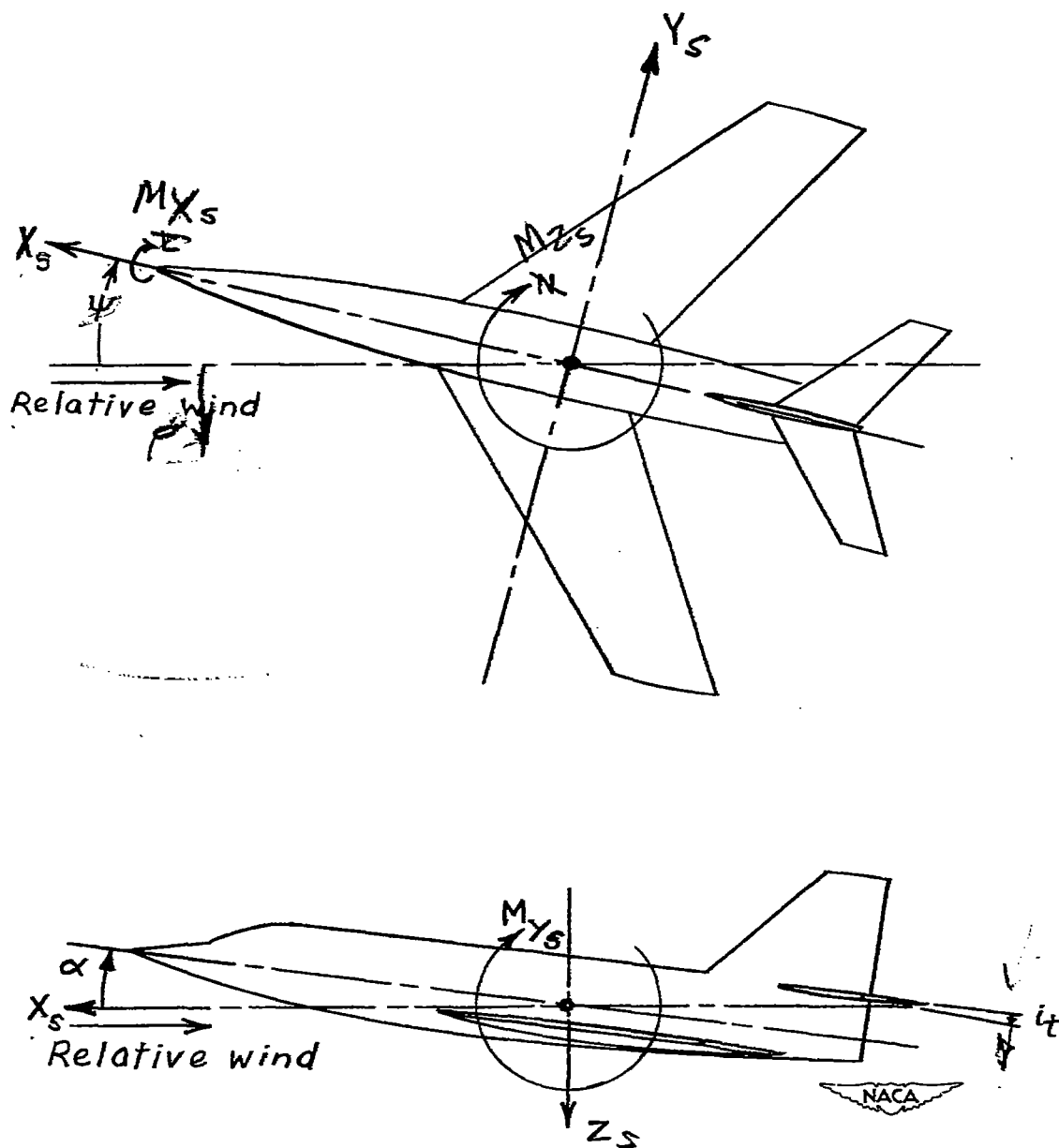


Figure 1.- System of stability axes. Arrows indicate positive values.

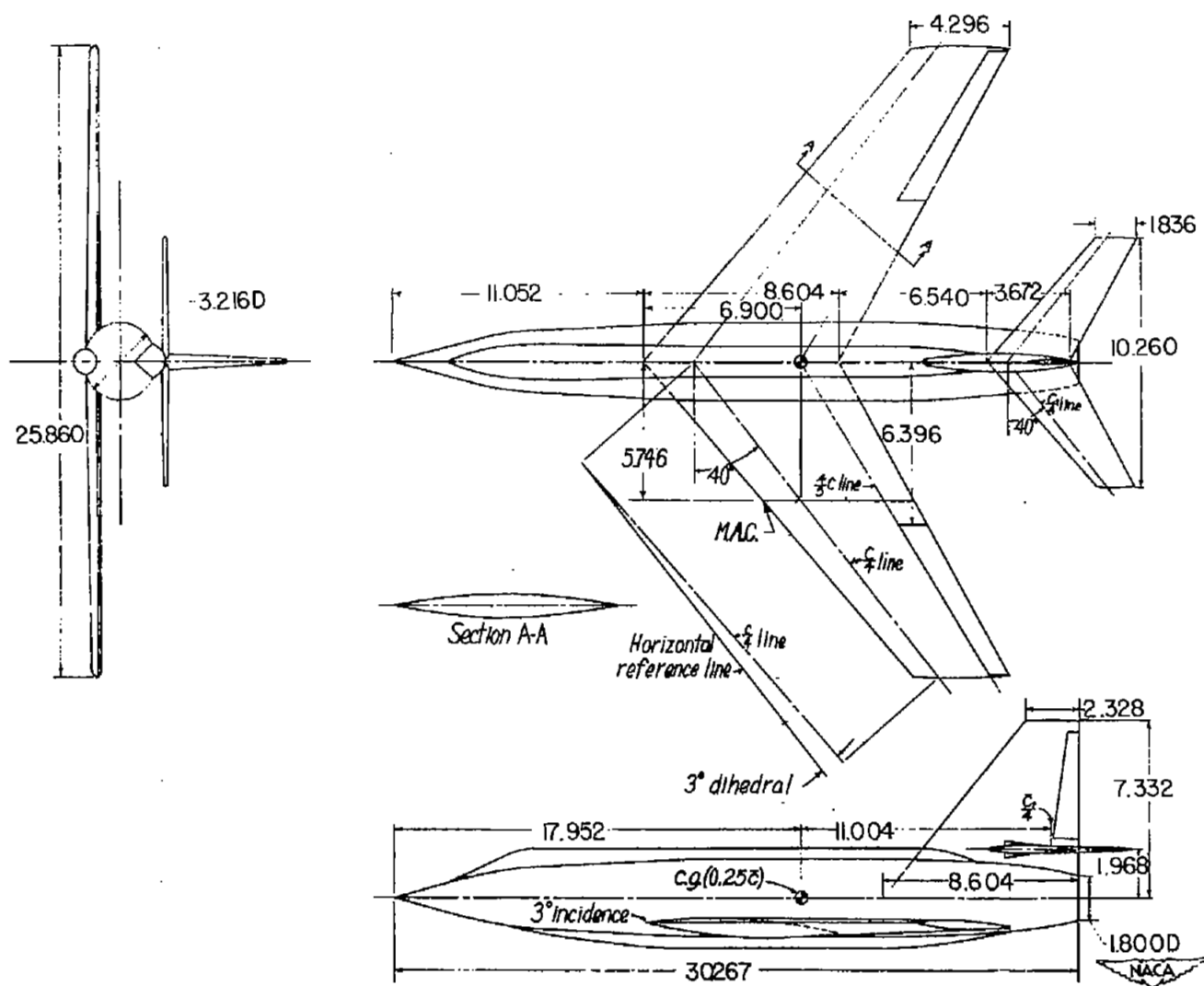


Figure 2.- Details of model of supersonic aircraft configuration.  
Dimensions in inches unless otherwise noted.



Figure 3.- Model installation in the test section of the Langley 4-  
by 4-foot supersonic tunnel.



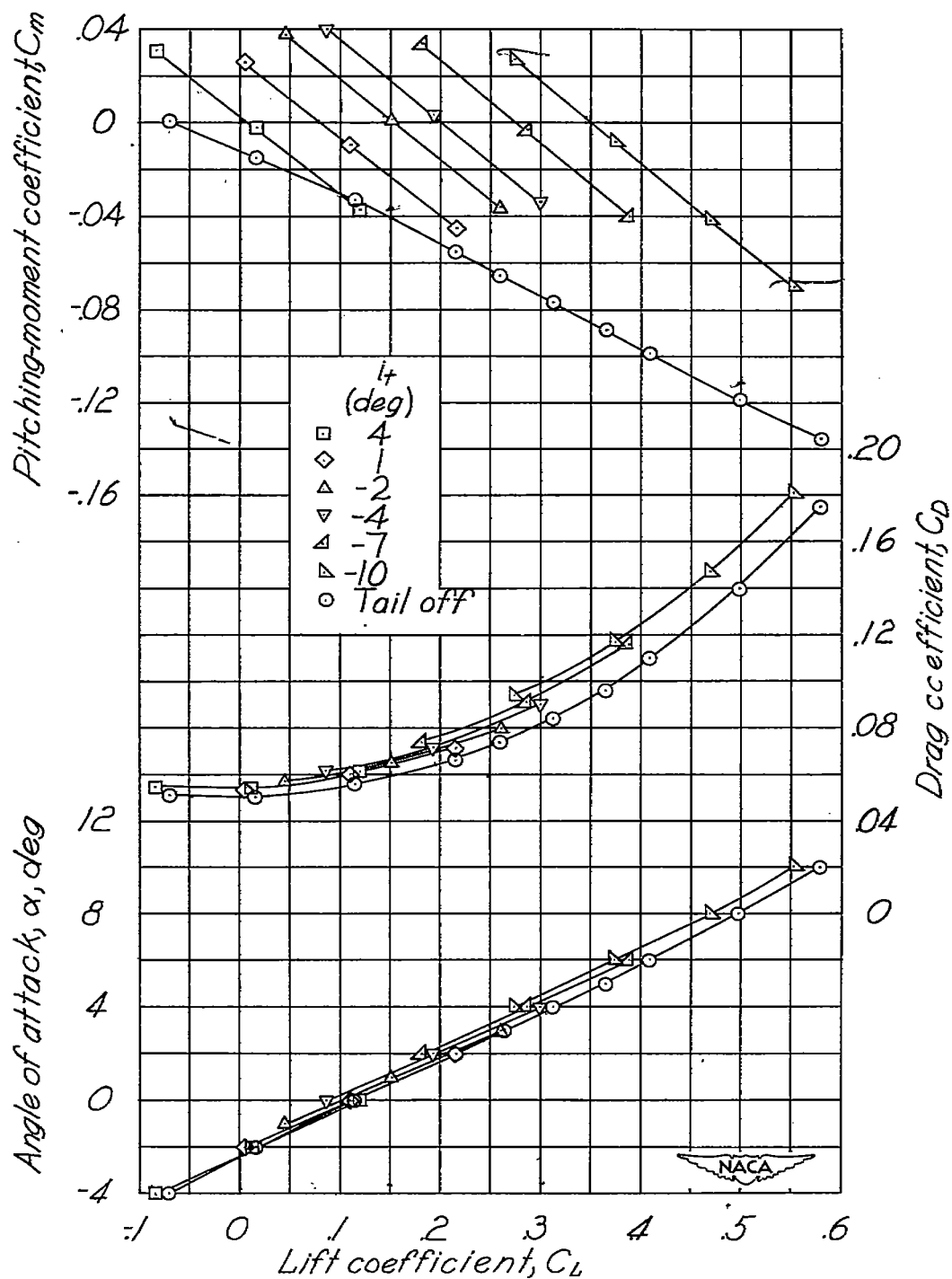
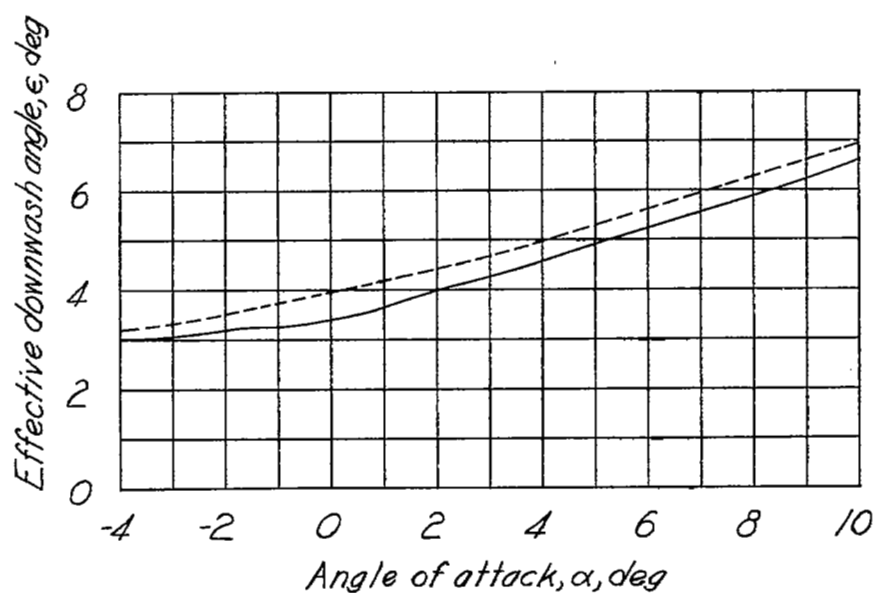
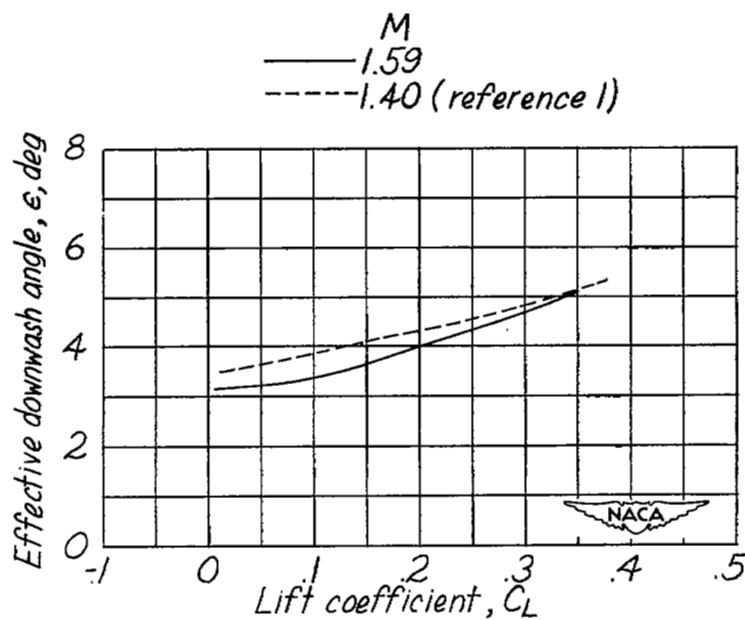


Figure 4.- Effect of stabilizer deflection on the aerodynamic characteristics in pitch.  $M = 1.59$ .





(a)  $\epsilon$  plotted against  $\alpha$ .



(b)  $\epsilon$  plotted against  $C_L$ .

Figure 5.- Variation of effective downwash angle with angle of attack and lift coefficient.

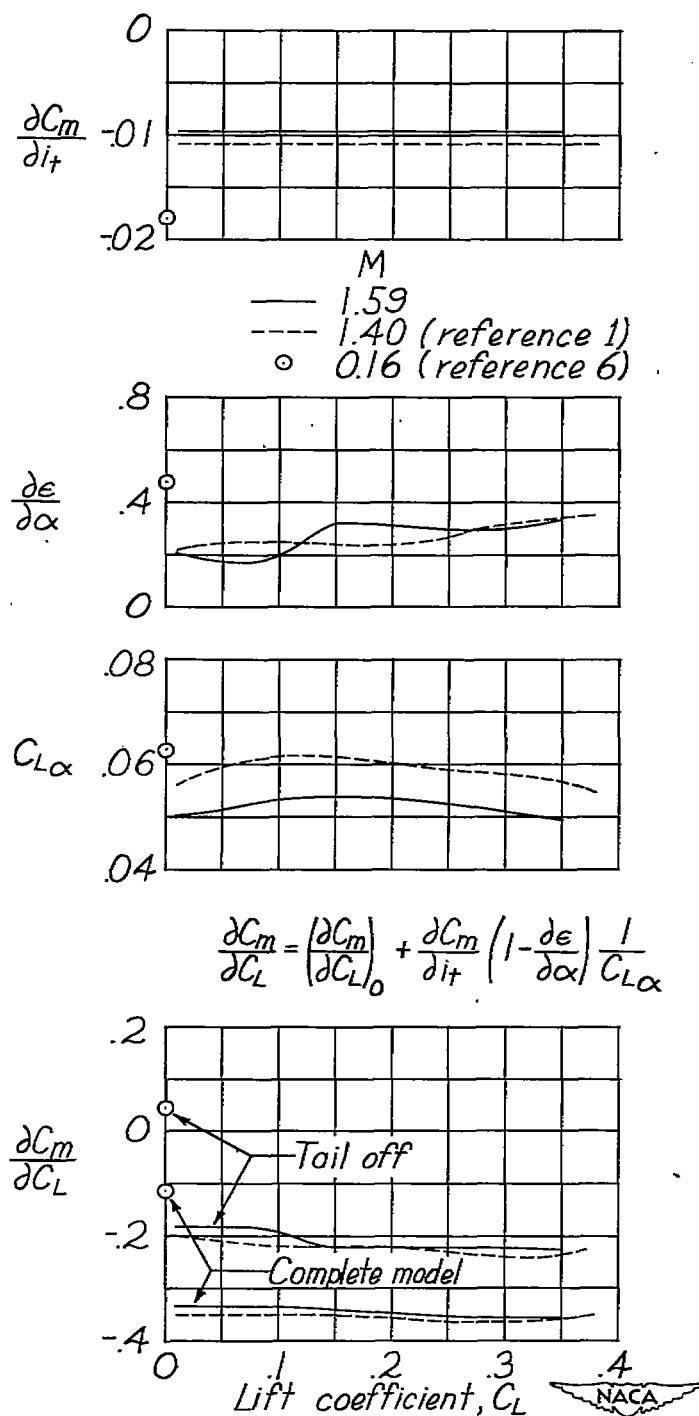


Figure 6.- Variation of the static-longitudinal-stability determinants with lift coefficient.

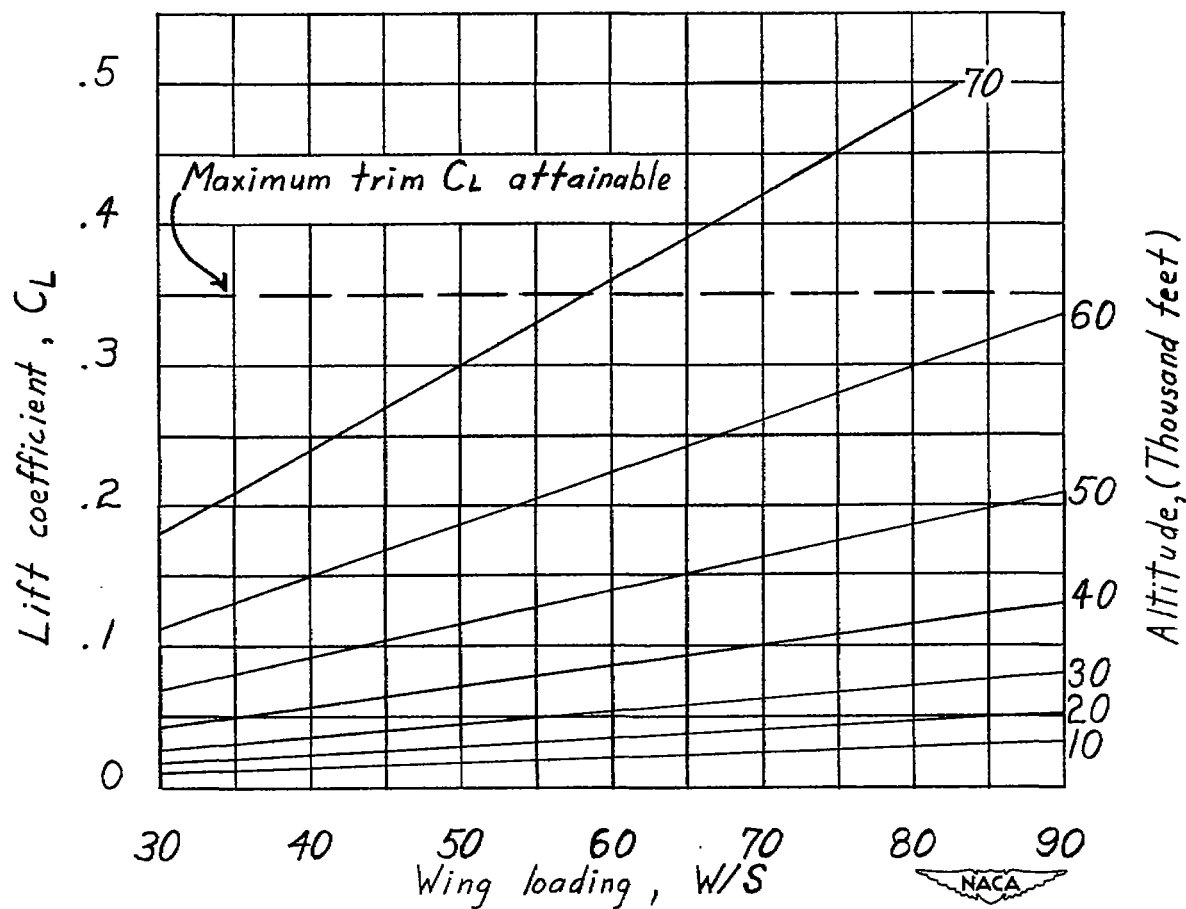
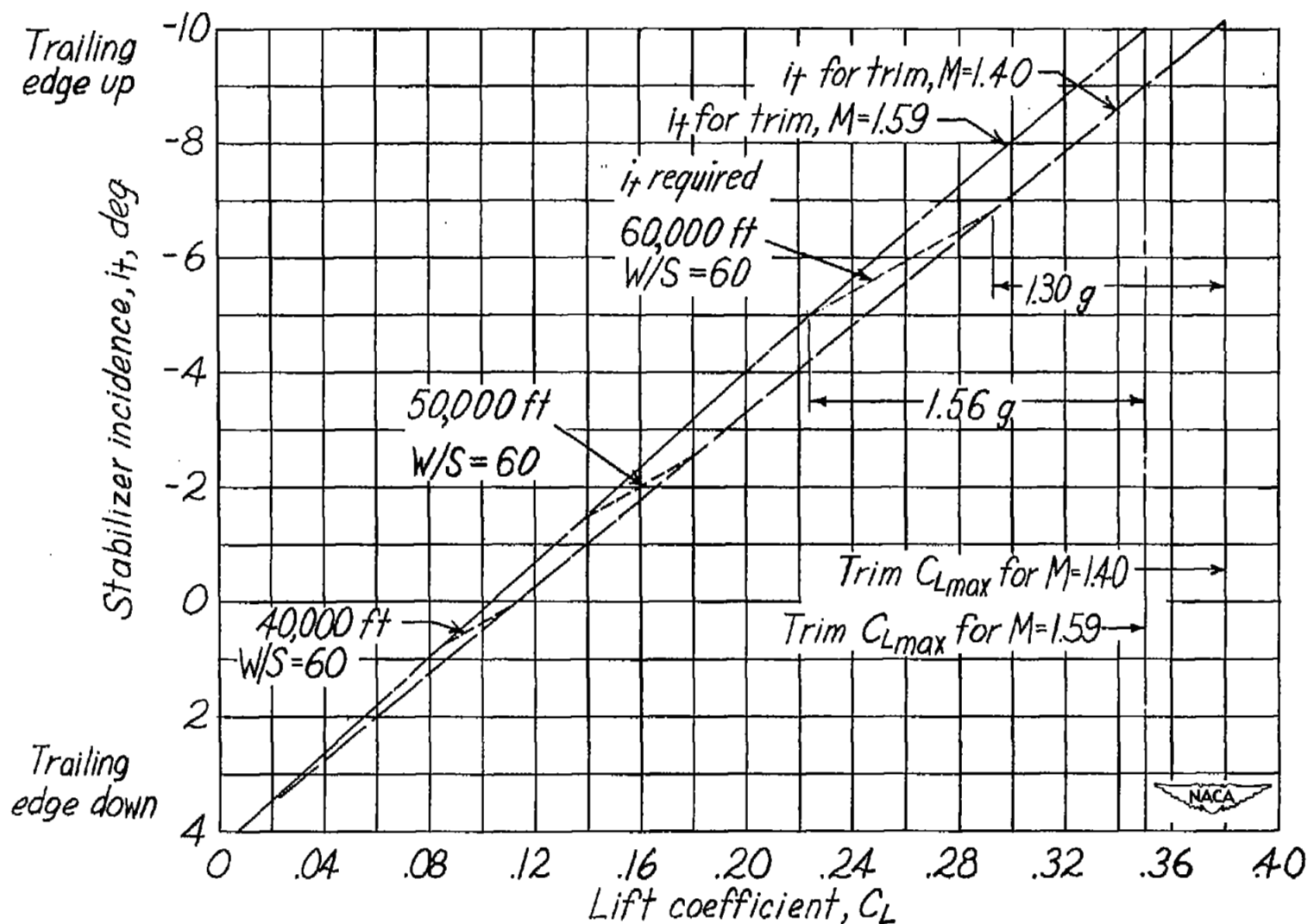


Figure 7.- Variation with wing loading and altitude of the lift coefficient required for trimmed level flight.  $M = 1.59$ .

Figure 8.- Longitudinal control characteristics for  $M = 1.40$  and  $1.59$ .

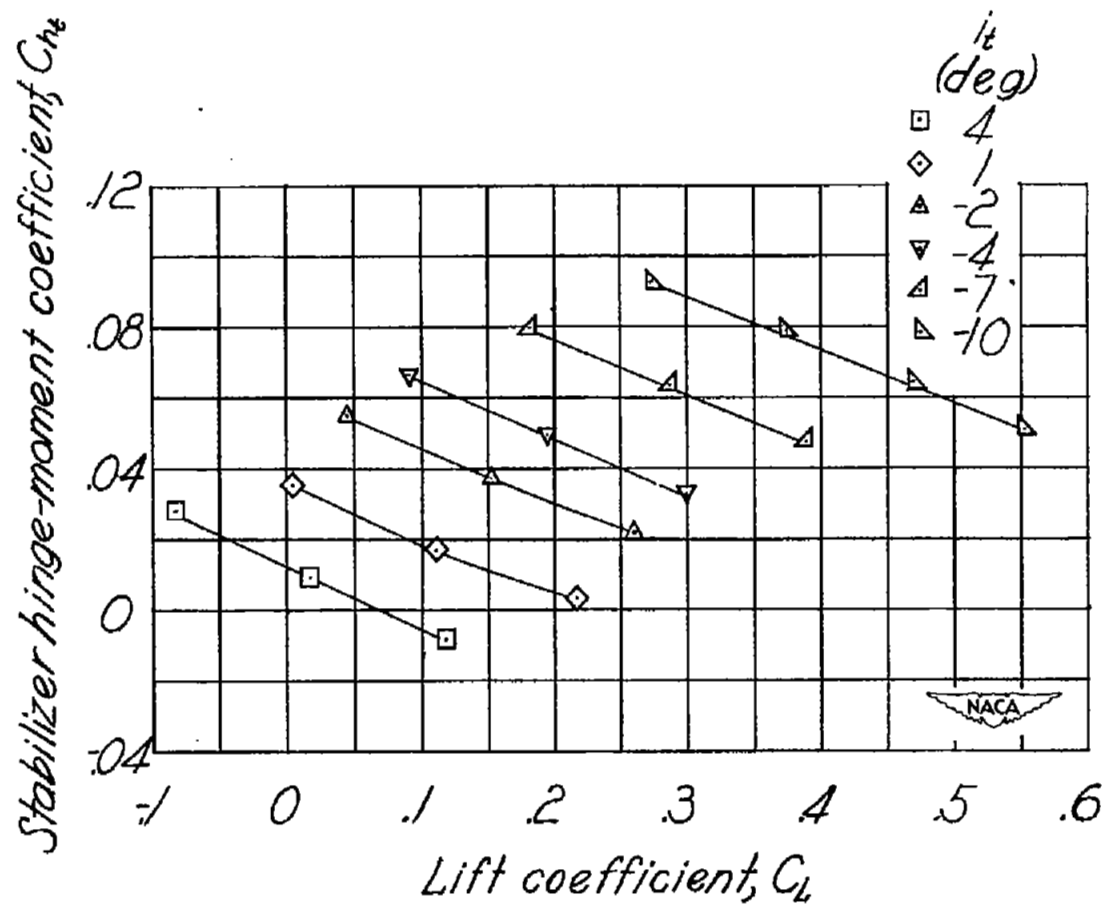


Figure 9.- Effect of stabilizer deflection on the stabilizer hinge-moment coefficient.  $M = 1.59$ .

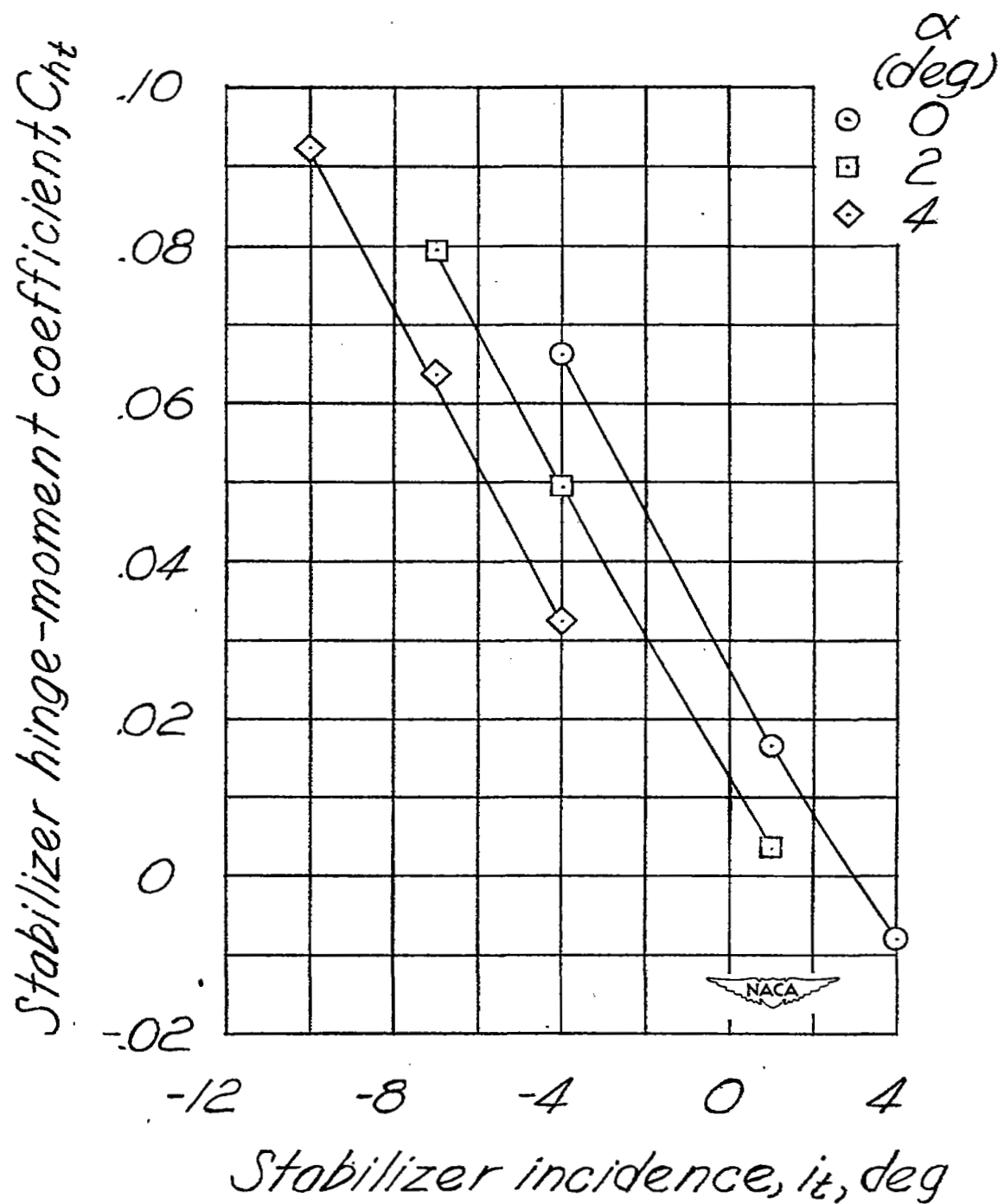


Figure 10.- Variation of stabilizer hinge-moment coefficient with stabilizer incidence.  $M = 1.59$ .

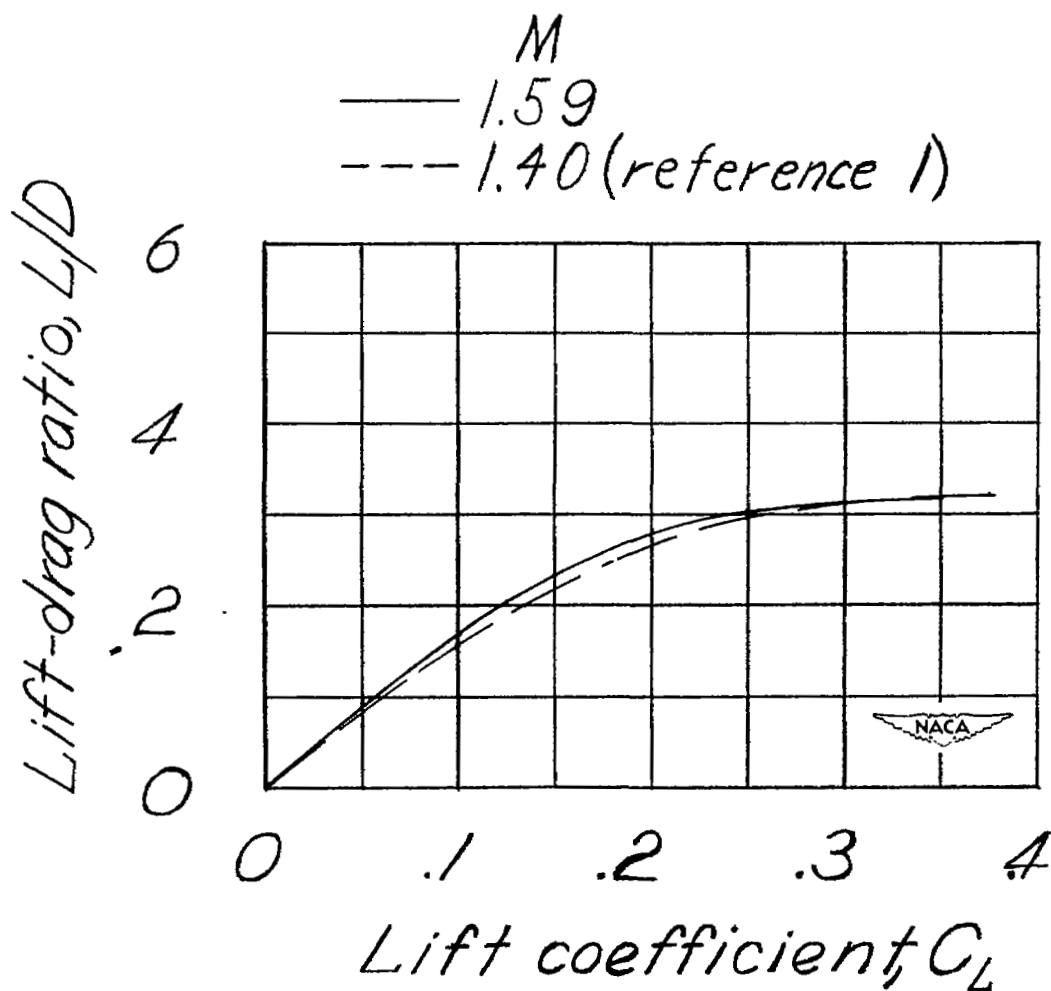


Figure 11.- Variation of lift-drag ratio with lift coefficient.

